Am J Physiol Renal Physiol 281: F1092–F1101, 2001.
First published August 8, 2001; 10.1152/ajprenal.00091.2001.

Rho inhibits cAMP-induced translocation of aquaporin-2 into the apical membrane of renal cells

GRAZIA TAMMA,[1] ENNO KLUSSMANN,[2] KENAN MARIC,[2] KLAUS AKTORIES,[3] MARIA SVELTO,[1] WALTER ROSENTHAL,[2,4] AND GIOVANNA VALENTI[1]
[1]*Università di Bari, Dipartimento di Fisiologia Generale e Ambientale, 70126 Bari, Italy;* [2]*Forschungsinstitut für Molekulare Pharmakologie, Campus Berlin-Buch, 13125 Berlin;* [3]*Institut für Pharmakologie und Toxikologie, Albert-Ludwigs-Universität Freiburg, 79104 Freiburg; and* [4]*Institut für Pharmakologie, Freie Universität Berlin, 14195 Berlin, Germany*

Received 16 March 2001; accepted in final form 6 August 2001

Tamma, Grazia, Enno Klussmann, Kenan Maric, Klaus Aktories, Maria Svelto, Walter Rosenthal, and Giovanna Valenti. Rho inhibits cAMP-induced translocation of aquaporin-2 into the apical membrane of renal cells. *Am J Physiol Renal Physiol* 281: F1092–F1101, 2001. First published August 8, 2001; 10.1152/ajprenal.00091.2001.—We have recently demonstrated that actin depolymerization is a prerequisite for cAMP-dependent translocation of the water channel aquaporin-2 (AQP2) into the apical membrane in AQP2-transfected renal CD8 cells (29). The Rho family of small GTPases, including Cdc42, Rac, and Rho, regulates the actin cytoskeleton. In AQP2-transfected CD8 cells, inhibition of Rho GTPases with *Clostridium difficile* toxin B or with *C. limosum* C3 fusion toxin, as well as incubation with the Rho kinase inhibitor, Y-27632, caused actin depolymerization and translocation of AQP2 in the absence of the cAMP-elevating agent forskolin. Both forskolin and C3 fusion toxin-induced AQP2 translocation were associated with a similar increase in the osmotic water permeability coefficient. Expression of constitutively active RhoA induced formation of stress fibers and abolished AQP2 translocation in response to forskolin. Cytochalasin D induced both depolymerization of F-actin and AQP2 translocation, suggesting that depolymerization of F-actin is sufficient to induce AQP2 translocation. Together, these data indicate that Rho inhibits cAMP-dependent translocation of AQP2 into the apical membrane of renal principal cells by controlling the organization of the actin cytoskeleton.

aquaporin; C3 toxin; toxin B; actin cytoskeleton; G proteins; adenosine 3′,5′-cyclic monophosphate

IN RENAL PRINCIPAL CELLS, the antidiuretic hormone arginine-vasopressin (AVP) regulates the shuttling of the water channel AQP2 from intracellular vesicles into the plasma membrane (8, 14, 34). AVP binds vasopressin V_2 receptors coupled to the G_s-adenylyl cyclase system. Activation of this system results in the activation of protein kinase A (PKA), which induces phosphorylation of AQP2 at Ser^{256} (10, 12). The phosphorylation of AQP2 by PKA and also the anchoring of PKA to subcellular compartments via protein kinase A anchoring proteins (AKAPs) are prerequisites for AQP2 translocation to the cell membrane (11, 12).

F-actin has been demonstrated to be involved in AVP-mediated changes of osmotic water permeability (3, 4, 12, 28). Depolymerization of cortical F-actin has been considered an important prerequisite for exocytosis. Calcium/ATP causes cortical F-actin disassembly (calmodulin dependent) and secretion (calmodulin independent) in permeabilized mast cells (25). Thus the cortical actin network may represent a cage that blocks the exocytotic process, and its disassembly constitutes an early stage of this reaction. In toad bladder, a renal-like epithelium, as well as in rat collecting duct epithelium, the total F-actin content decreases by 20–30 and 26%, respectively, after stimulation with vasopressin (5, 24). In AQP2-transfected renal collecting duct cells (CD8 cells), okadaic acid, an inhibitor of 1 and 2A phosphatases, induces actin depolymerization, leading to AQP2 translocation in the absence of cAMP-elevating agents (29).

Proteins of the Rho family (Cdc42, Rac, and Rho) are involved in the regulation of F-actin polymerization. Activation of Rho triggers the assembly of actin stress fibers and formation of focal adhesions, whereas activation of Rac leads to formation of lamellipodia and membrane ruffles, and activation of Cdc42 induces surface protrusions (filopodia) (1, 7, 31). In permeabilized mast cells, inhibition of Rho by *Clostridium botulinum* C3 toxin prevented Ca^{2+}-triggered secretion of hexoseaminidase (25), whereas constitutively active RhoA or Rac greatly enhanced Ca^{2+}-induced secretion (22).

In this study, we investigated the hypothesis that proteins of the Rho family may be involved in the control of AQP2 translocation to the cell membrane. The rabbit cortical collecting duct cell line CD8, stably transfected with rat AQP2 (CD8 cells; Ref. 27), was utilized to test this hypothesis.

The results obtained demonstrate that the selective inhibition of Rho or inhibition of its effectors, the Rho

Address for reprint requests and other correspondence: G. Valenti, Dipartimento di Fisiologia Generale e Ambientale, Via Amendola 165/A, 70126 Bari, Italy (E-mail: g.valenti@biologia.uniba.it).

The costs of publication of this article were defrayed in part by the payment of page charges. The article must therefore be hereby marked "*advertisement*" in accordance with 18 U.S.C. Section 1734 solely to indicate this fact.

kinases, caused actin depolymerization and translocation of AQP2 into the cell membrane in the absence of the cAMP-elevating agent forskolin. Rho inhibition resulted in an increase of the osmotic water permeability coefficient (P_f), indicating a functional insertion of AQP2 into the plasma membrane.

METHODS

Materials. C. difficile toxin B (17) and *C. limosum* C3 fusion toxin (2) were prepared as described. To allow C3 fusion toxin internalization into CD8 cells, a recombinant toxin was generated consisting of full-length *C. limosum* C3 fusion toxin fused to the (inactive) NH_2-terminal part of the actin-ADP-ribosylating C2I component of the *C. botulinum* binary toxin C2 (C3 fusion toxin; C2IN-C3; Ref. 2). Coincubation of C3 fusion toxin with the activated membrane-binding component C2II of *C. botulimum* C2 toxin facilitates uptake of the C3 fusion toxin into cells via receptor-mediated endocytosis. Y-27632, the specific Rho kinase inhibitor, was kindly provided by Welfide (Osaka, Japan; Ref. 9, 26).

FITC-conjugated phalloidin was purchased from Sigma-Aldrich (Milan, Italy). AQP2 was detected with a polyclonal antiserum raised against the COOH terminus of rat AQP2 (27, 30).

CD8 cell culture. CD8 cells were cultured as described (27, 29, 30) and incubated with toxins as indicated. As control, the cAMP-mediated translocation of AQP2 was induced by incubation of CD8 cells with forskolin (100 μM, 15 min at 37°C).

CD8 cell transfection with RhoA-V14-GFP. CD8 cells were grown on glass coverslips for 15–18 h (subconfluent) and then transiently transfected with the plasmid encoding a fusion protein (RhoA-V14-GFP) of constitutively active RhoA (RhoA-V14) and green fluorescent protein (GFP; Ref. 13). Lipofectin (10 μg; Life Technologies, San Giuliano Milanese, Italy) was diluted in 2 ml of serum-free medium containing 2.8 μg of plasmid DNA. The mixture was added to the cells, incubated for 12 h, and replaced with normal medium supplemented with 5% newborn calf serum. Cells were processed for immunofluorescence microscopy after 2 additional days of growth (see below).

Immunofluorescence microscopy and quantification of immunofluorescence intensities. AQP2 was detected by epifluorescence microscopy (Leica DMRXA microscope) using specific antibodies and FITC-conjugated anti-rabbit secondary antibodies. Digital images were obtained using a cooled charge-coupled device (CCD) camera (Princeton Instruments). Immunofluorescence signals were detected in the basal planes of the cells (27). RhoA-V14-GFP expression was visualized by detection of GFP fluorescence using epifluorescence microscopy. For visualization of F-actin, CD8 cells were grown, fixed, and incubated with phalloidin-FITC (100 μg/ml, 30 min; Ref. 29). The F-actin cytoskeleton was visualized by epifluorescence microscopy (Leica microscope with CCD camera).

Quantification of the effects of the toxins and of RhoA-V14 expression on AQP2 localization was performed as described previously (29, 30). Briefly, the statistical parameter skewness was calculated for images obtained from the basal planes of the cells by epifluorescence microscopy using identical exposure times for each set of experiments. Skewness can be regarded as an index of AQP2 redistribution (29, 30) and is a measure of the symmetry of a profile about the mean pixel intensity value. For all groups, mean and SE values were calculated, and statistical analysis was carried out using Student's *t*-test.

Laser scanning reflection microscopy and analysis of permeability coefficient changes in single cells. Laser scanning reflection microscopy (LSRM; Ref. 19) was applied to determine osmotic water permeability coefficient changes in epithelial cells grown on glass coverslips. The experimental bathing solutions were obtained by replacing the bicarbonate-CO_2-based buffer of the culture media system by HEPES-buffer (10 mM), and FCS was replaced by sorbitol to adjust the osmolality to 300 mosmol/kgH_2O. This normotonic bathing *solution N* was diluted with distilled water to obtain hypotonic *solution H* (100 mosmol/kgH_2O). CD8 cells were cultured until they reached a subconfluent density, washed twice with the appropriate bathing *solution N* (300 mosmol/kgH_2O), and mounted in a custom-made metal cuvette into the motor-driven *x-y* table of the microscope (LSM 410, Zeiss).

The cell-swelling reaction and data acquisition were performed as described (19). Briefly, cells were selected using the transmission mode of the LSM 410, and thereafter the optical setting of the LSM 410 was changed to the reflection mode. Cells were scanned with a ×63 magnification water-immersion objective with a numerical aperture of 1.2. The initially applied bathing *solution N* was removed by suction. Cell swelling was then initiated by the application of bathing *solution H*. *X-z*-scans were recorded with a frequency of 0.25 Hz and stored as a time series. Thereafter, cells were allowed to recover in bathing *solution N*. For this purpose, they were placed inside the metal cuvette on a precision heating block (Precitherm). During this period, cells were left either untreated or stimulated as indicated. After the exchange of bathing solutions from *N* to *H*, swelling of the identical cells was recorded for a second time, as described above.

The time constants of the swelling processes before (τ_0) and after (τ^*) the indicated treatments were then delineated from the increases in vertical section areas (a) for each cell as described (19). The quotients of τ^*/τ_0 reflect the inverse increase in the cells' P_f. The mean P_f increases in single cells ($10 < n < 12$) were then compared by one-way ANOVA and Bonferroni's multiple comparison test, as well as by a histogram analysis after an automatic binning procedure, using the GraphPad Prism software for Windows (version 3.00).

RESULTS

Effects of bacterial toxins and of the Rho kinase inhibitor Y-27632 on the F-actin cytoskeleton. CD8 cells were treated with bacterial toxins affecting the activity of GTP-binding proteins of the Rho family. To test the effect of the toxins on F-actin organization, CD8 cells were cultured for 3 days and incubated with toxin B (200 ng/ml, 2 h), with C3 fusion toxin (100 ng/ml) and C2II (200 ng/ml, 4 h), or, as a control, with the catalytically active C3 fusion toxin (100 ng/ml, 4 h) in the absence of C2II, which is required for cellular uptake of the toxin. In additon, CD8 cells were incubated with Y-27632 (100 mM, 1 h). As controls, CD8 cells were left untreated or stimulated with forskolin (100 μM, 15 min). After these treatments, cells were fixed, permeabilized, and incubated with FITC-conjugated phalloidin (0.1 mg/ml, 30 min), and F-actin was visualized by epifluorescence microscopy.

Toxin B and the coincubation of C3 fusion toxin and C2II induced a strong reduction in F-actin content comparable to that observed after forskolin stimulation (Fig. 1). C3 fusion toxin in the absence of the

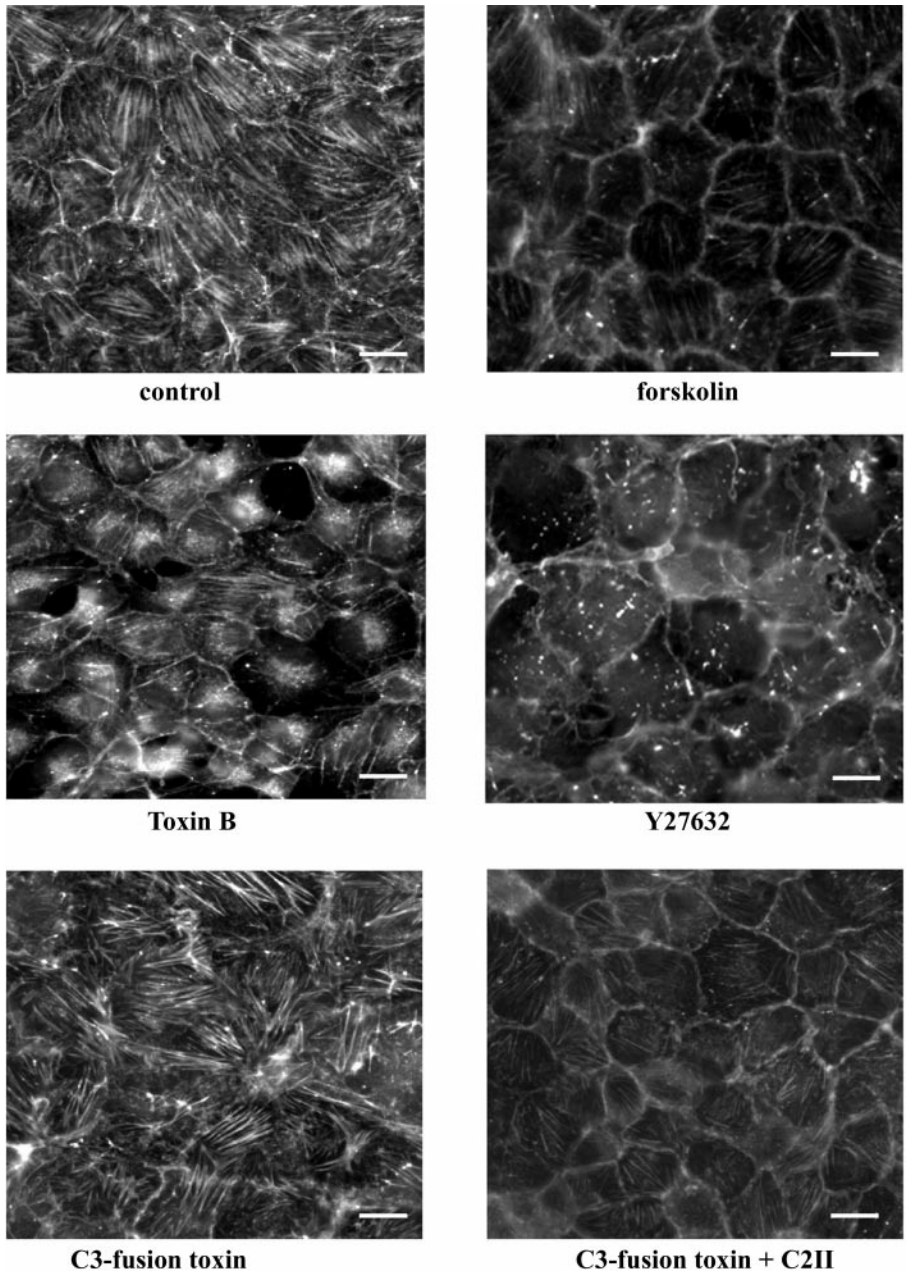

Fig. 1. Effect of bacterial toxins and Y-27632 on the F-actin cytoskeleton. CD8 cells were left untreated (control), stimulated with forskolin (100 μM, 15 min), or incubated with toxin B (200 ng/ml, 2 h), the catalytically active C3 fusion toxin alone (100 ng/μl, 4 h), both C3 fusion toxin (100 ng/μl, 4 h) and the membrane-binding component C2II (200 ng/μl, 4 h), or the Rho kinase inhibitor Y-27632 (100 mM, 1 h). After incubations for the indicated lengths of time, cells were fixed, permeabilized, and incubated with FITC-conjugated phalloidin (0.1 mg/ml). Fluorescence was detected by epifluorescence microscopy. Results shown are representative of at least 3 separate experiments. Scale bars, 20 μm.

membrane-binding component C2II had no effect (Fig. 1). Incubation of cells with toxin B, with C3 fusion toxin and C2II, or with Y-27632 resulted in the disappearance of intracellular F-actin, apparently without affecting cortical F-actin (Fig. 1). Thus the toxins were effective in altering F-actin-containing structures, i.e., the stress fibers at the concentration used.

Inibition of the Rho family proteins and Rho alone results in a relocalization of AQP2 to the apical cell membranes in the absence of cAMP-elevating agents. Toxin B was applied to investigate whether Rho, Rac, and Cdc42 were involved in the regulation of AQP2 translocation. CD8 cells were incubated with toxin B to inactivate the Rho family proteins, and the distribution of AQP2 was determined by immunofluorescence microscopic analysis using specific antisera. Figure 2 shows epifluorescence microscopic images taken in the basal plane of the cells. In untreated CD8 cells (control), AQP2 was localized intracellularly, indicated by the bright punctate staining around the nuclei. In contrast, AQP2 staining is drastically reduced in the basal plane of the cells after treatment with forskolin or toxin B due to a redistribution of AQP2 into the apical cell membrane (27, 29). The effects of forskolin and toxin B were quantified using the parameter skewness for the basal planes of the cells (Fig. 3; Refs. 29, 30). The statistical parameter of skewness can be regarded as an index of AQP2 redistribution (29, 30). In nonstimulated cells, the value for skewness was 1.42 ± 0.013 (means ± SE; Fig. 3), indicating a predominant intracellular localization of AQP2. In forskolin-stimulated and in toxin B-treated

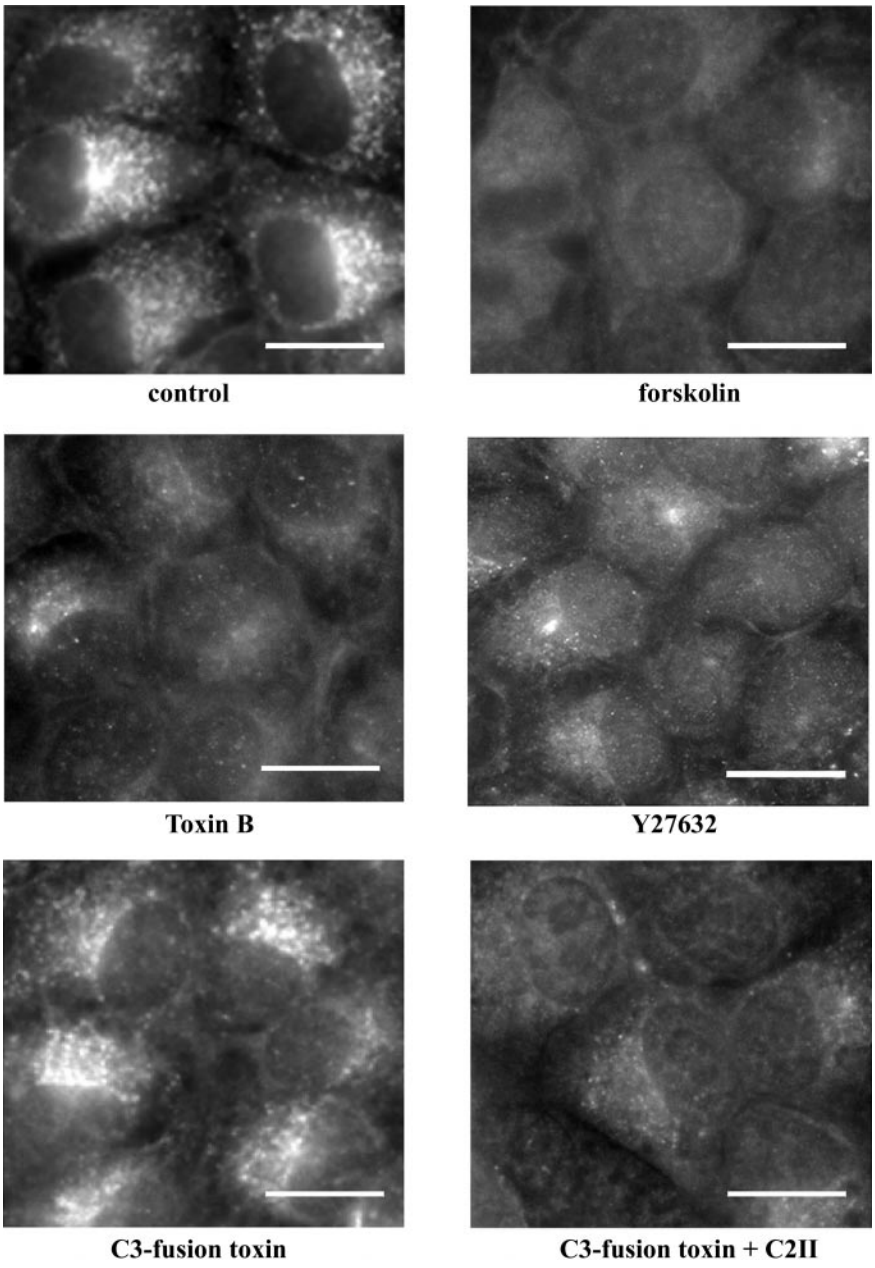

Fig. 2. Immunolocalization of aquaporin-2 (AQP2) in CD8 cells. Cells were left untreated (control), stimulated with forskolin (100 μM, 15 min), or incubated with toxin B (200 ng/ml, 2 h), the catalytically active C3 fusion toxin alone (100 ng/μl, 4 h), both C3 fusion toxin (100 ng/μl, 4 h) and the membrane-binding component C2II (200 ng/μl, 4 h), or Y-27632 (100 μM, 1 h). The cells were fixed, permeabilized, and incubated with anti-AQP2 and secondary FITC-conjugated anti-rabbit antibodies. Immunofluorescence was monitored by epifluorescence microscopy. Images were taken from the basal planes of the cells. Results shown are representative of at least 3 separate experiments. Scale bars, 20 μm.

cells, the values were 2.75 ± 0.12 and 2.18 ± 0.09, respectively. These values were significantly different from the unstimulated control (Fig. 3), indicating a predominant localization of AQP2 in the cell membrane. These results suggest that inhibition of the protein of the Rho family causes AQP2 redistribution to the apical cell membrane, whereby constitutive membrane localization of AQP2 is prevented in resting CD8 cells.

To analyze which protein of the Rho family might be responsible for the inhibition of AQP2 translocation in resting CD8 cells, C3 fusion toxin, which specifically inactivates Rho, was used (see METHODS; Ref. 2). Coincubation with C3 fusion toxin and C2II induced a strong translocation of AQP2 into the apical cell membranes (Fig. 2), whereas incubation with C3 fusion toxin alone had no effect on the localization of AQP2 (Fig. 2). Inhibition of the downstream effectors of Rho, the Rho kinases, by Y-27632 (9, 26) also induced a translocation of AQP2 to the cell membrane (Fig. 2). Quantitative analysis of the effect of coincubation with C3 fusion toxin and C2II on CD8 cells (Fig. 3) revealed a value of 2.32 ± 0.12 for skewness, which was significantly different from that obtained for nonstimulated control cells. Moreover, treatment with Y-27632 revealed an induction of AQP2 translocation similar to that found for the tested toxins (skewness value 1.94 ± 0.07, significantly different from the control; Fig. 3). These data suggest that, in resting cells, a Rho-dependent pathway is involved in preventing a constitutive membrane localization of AQP2.

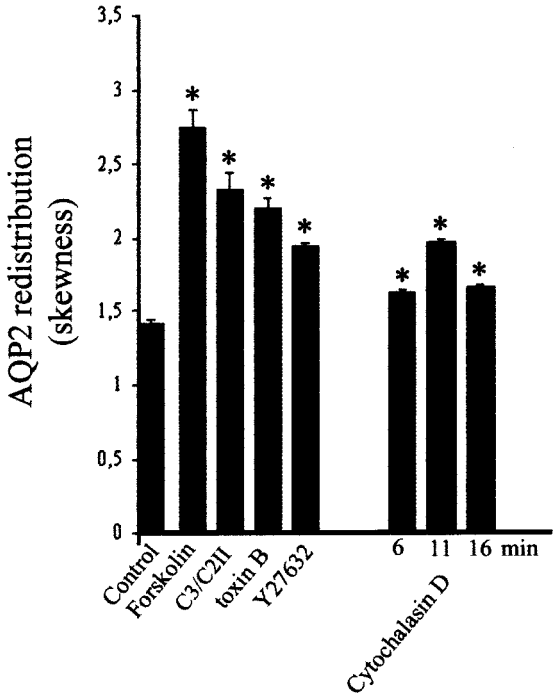

Fig. 3. Semiquantification of AQP2 redistribution by image analysis. Cells were incubated as described in the legend to Figs. 1, 2, 4, 5, and 6. Immunofluorescence signals were visualized, the distribution of pixel intensity as a function of their frequency was determined for each image, and the statistical parameter of skewness was calculated (see METHODS). The statistical parameter of skewness can be regarded as an index of AQP2 redistribution (29, 30). Each column represents the mean ± SE of the parameters obtained from at least 4 randomly chosen boxes from different fields of the coverslip from 3 different experiments. Statistically significant differences from untreated control cells are indicated (*$P < 0.001$).

Constitutively activated Rho abolishes forskolin-mediated translocation of AQP2 into the cell membrane of CD8 cells. Because the reported data indicate that inhibition of Rho or Rho kinases causes the translocation of AQP2 to the cell membrane in resting CD8 cells (Figs. 2, 3), we investigated the effect of constitutively active Rho on AQP2 redistribution in response to elevation of intracellular cAMP. For this purpose, CD8 cells were transiently transfected with a plasmid encoding constitutively active RhoA (RhoA-V14) fused to the GFP. RhoA-V14-expressing cells were visualized by detection of GFP fluorescence. The activity of RhoA-V14 was assayed by its effect on actin stress fibers 48 h after transfection of CD8 cells. Figure 4*A* clearly shows that the mutant induced the formation of actin stress fibers in CD8 cells positive for the GFP. Expression of GFP alone had no effect on the localization of AQP2 (data not shown).

Figure 4*B* shows a representative nonstimulated RhoA-V14-expressing CD8 cell (GFP, control) in which AQP2 is localized intracellularly (AQP2, control). The righthand panels of Fig. 4*B* depict two representative forskolin-stimulated, RhoA-V14-expressing CD8 cells in which AQP2 is also localized intracellularly (*top*), whereas in the surrounding nontransfected cells AQP2 staining is strongly reduced due to redistribution of AQP2 to the apical cell membrane.

In none of the analyzed CD8 cells expressing RhoA-V14-GFP was AQP2 found in the cell membrane. It was therefore concluded that constitutively active RhoA-V14 prevents membrane localization of AQP2 in CD8 cells.

Cytochalasin D induces depolymerization of the F-actin cytoskeleton and translocation of AQP2 into the apical CD8 cell membranes. The data above show the involvement of Rho in the regulation of the intracellular localization of AQP2 in CD8 cells. To test whether Rho regulates the intracellular localization of AQP2 through regulation of F-actin-containing cytoskeletal structures, F-actin was depolymerized by incubation of cells with cytochalasin D (2 μM) for 6, 11, 16, 25, and 30 min. This treatment induced a gradual decrease in F-actin content over 0–25 min (Fig. 5). At early time points, AQP2 translocated to the cell membranes of

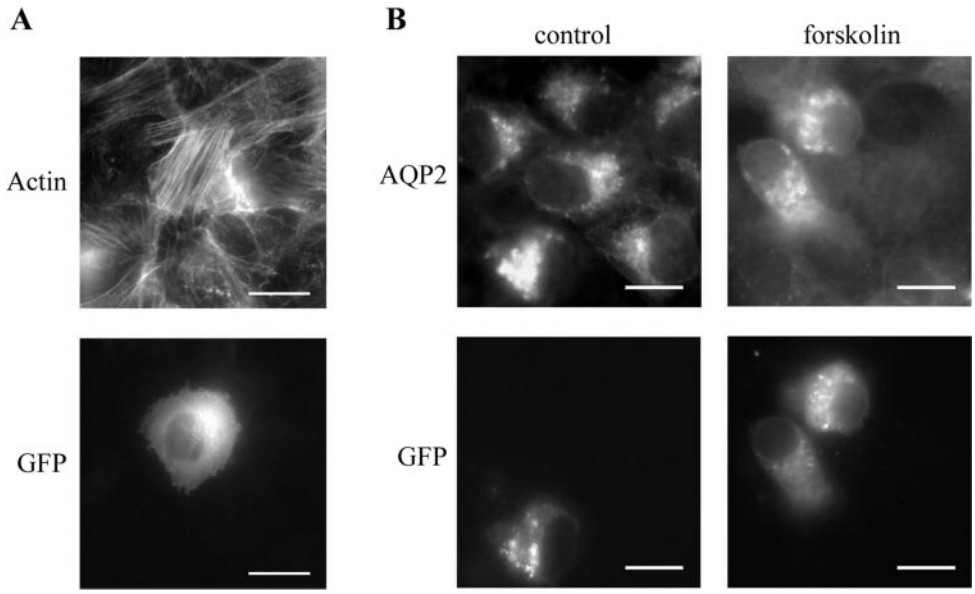

Fig. 4. Effect of the expression of a constitutively active mutant of RhoA (RhoA-V14) fused to the green fluorescent protein (GFP) on the F-actin cytoskeleton (actin) and on AQP2 localization in control and forskolin-stimulated (100 μM, 15 min) CD8 cells. *A*: cells were transiently transfected with the plasmid and analyzed for GFP expression 48 h after transfection (RhoA-V14-GFP). At this time point, the cells were fixed, permeabilized, and incubated with FITC-conjugated phalloidin to visualize F-actin (actin). *B*: detection of AQP2 and of RhoA-V14-GFP expression in nonstimulated (control) and forskolin-stimulated (forskolin, 100 μM, 15 min) CD8 cells 48 h after transfection. Results shown are representative of at least 4 separate experiments. Scale bars, 20 μm.

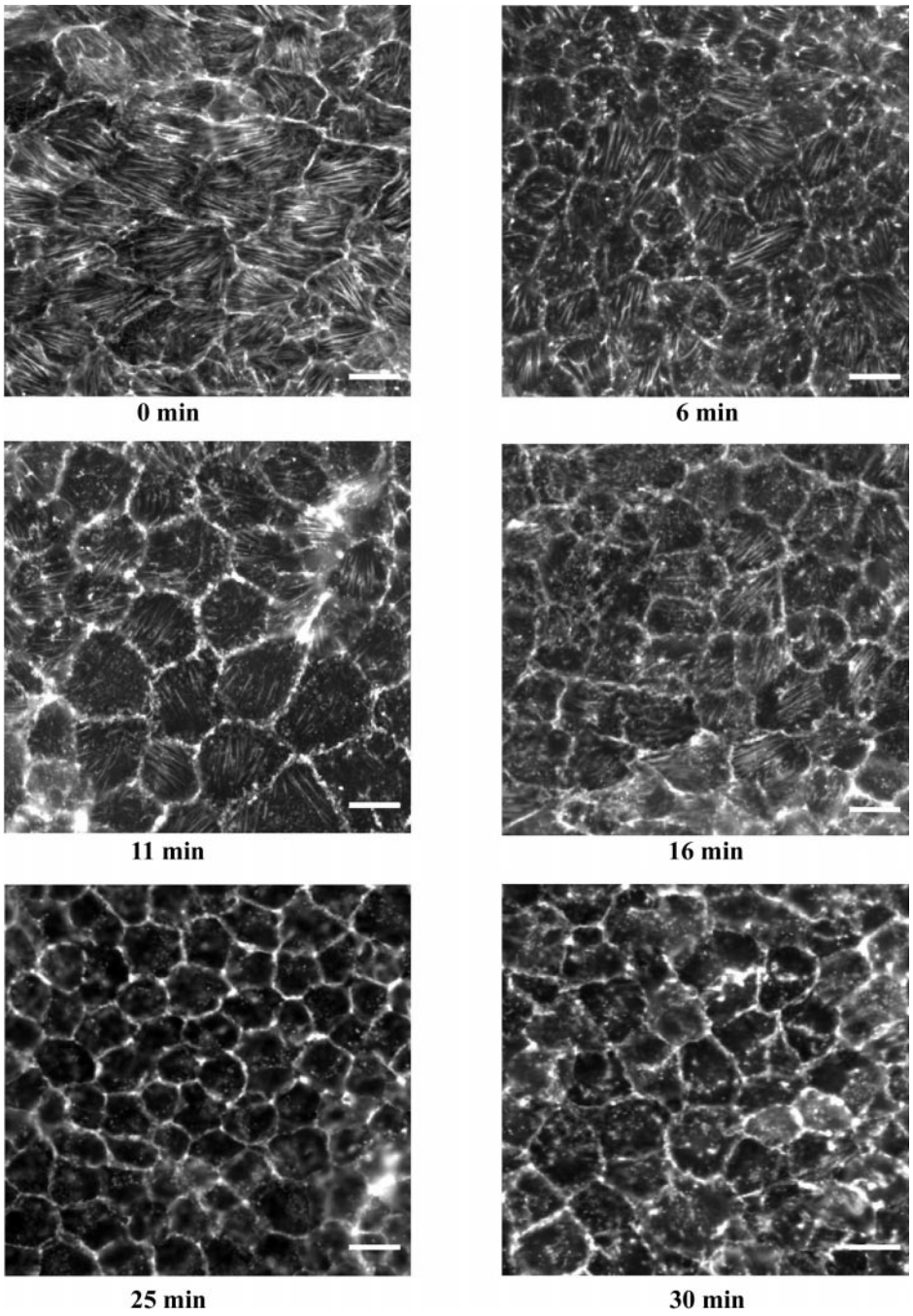

Fig. 5. The effect of cytochalasin D on the F-actin cytoskeleton in CD8 cells. Cells were left untreated (0 min) or incubated with cytochalasin D (2 μM), which induces F-actin depolymerization. At the time points indicated, the cells were fixed and F-actin was stained with FITC-conjugated phalloidin (0.1 mg/ml). Fluorescence was detected by epifluorescence microscopy. Results shown are representative of at least 3 separate experiments. Scale bars, 20 μm.

CD8 cells, as assessed by the disappearance of the intracellular staining from the basal plane (Fig. 6). Quantitative analysis of the effect of cytochalasin D on CD8 cells demonstrated values for skewness of 2.02 ± 0.08 and 2.28 ± 0.04 at 6 and 11 min, respectively, which indicates translocation of AQP2 to the cell membranes (Fig. 3). After 16 min of incubation with cytochalasin D, a skewness value of 2.06 ± 0.05 was obtained (Fig. 3). Longer incubation with cytochalasin D (25–30 min) severely affected cell shape and caused cell death. These results indicate that partial depolymerization of F-actin by cytochalasin D is sufficient to induce translocation of AQP2 to the cell membrane.

Selective inhibition of Rho increases the P_f in CD8 cells in the absence of forskolin stimulation. We investigated whether the observed redistribution of AQP2, after selective inhibition of Rho, results in an increase of the P_f. To this end, we applied a new method, LSRM (19), to analyze the changes of this biophysical property in single CD8 cells. The relationship of the time constants of the cell-swelling process initiated by replacing normotonic bathing *solution N* (300 mosmol/kgH_2O) with a hypotonic bathing *solution H* (100 mosmol/kgH_2O) before (τ_0) and after (τ^*) treatment of the cells reflects the changes in P_f in response to the chosen treatment. After an initial swelling, cells were

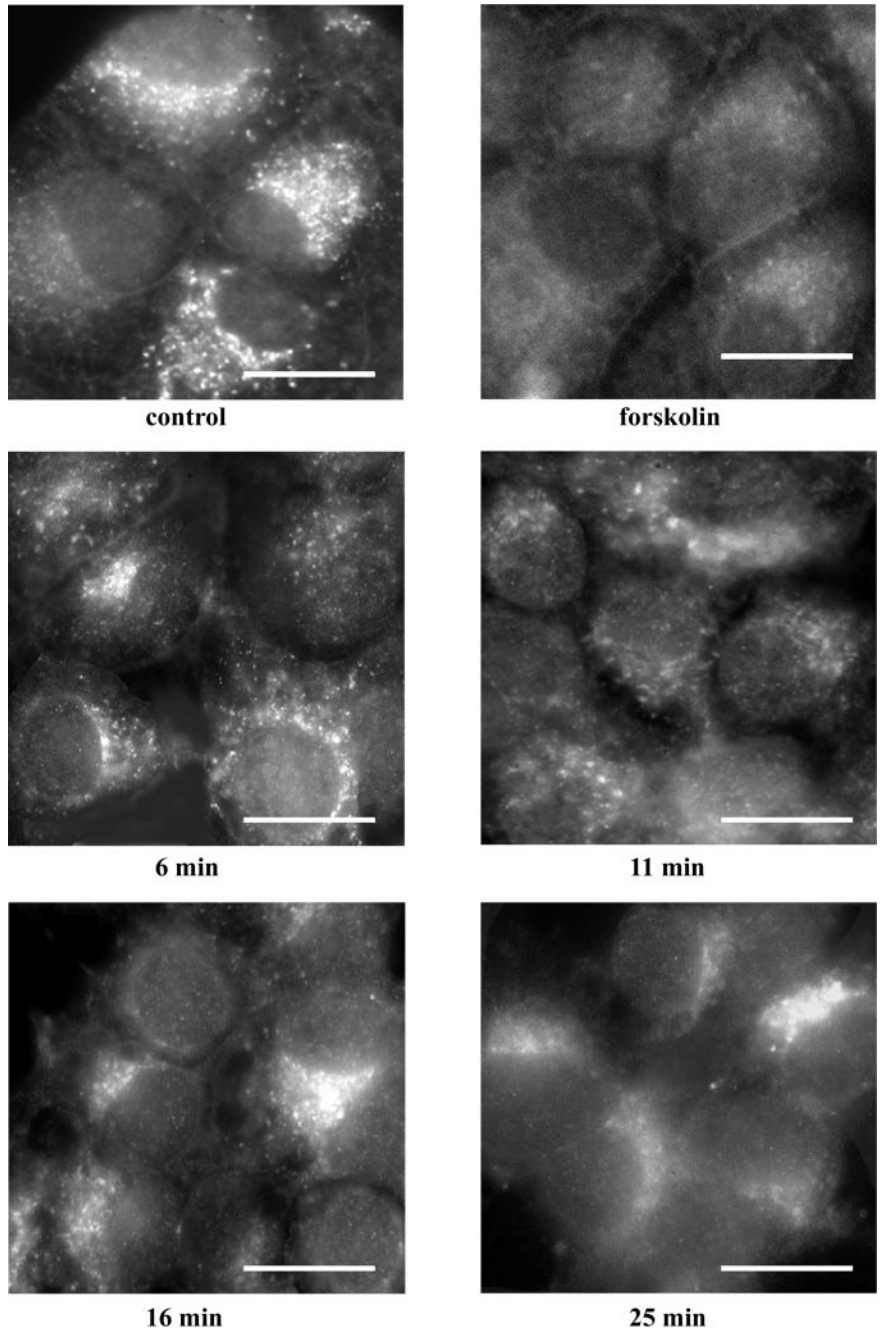

Fig. 6. Effect of cytochalasin D on the localization of AQP2 in CD8 cells. Cells were incubated with cytochalasin D (2 μM) for the indicated lengths of time. As controls, cells were incubated without (control) or with forskolin (100 μM, 15 min). Cells were fixed, permeabilized, and incubated with anti-AQP2 and secondary FITC-conjugated anti-rabbit antibodies. Immunofluorescence was visualized by epifluorescence microscopy. Images were taken along the basal plane of the cells. Results shown are representative of at least 3 separate experiments. Scale bars, 20 μm.

allowed to recover and either were left untreated or were treated with forskolin (100 μM, 15 min) or with a combination of C3 fusion toxin (100 ng/ml) and C2II (200 ng/ml, 4 h). After determination of τ^*, the quotient τ^*/τ_0 was calculated, which inversely describes the changes in the cells ($P_f = 1/P_f$ increase). This inversion was used because it exactly reflects the time constant after treatment as a function of the untreated condition [i.e., $\tau^* = \tau(\tau_0)$] as visualized by linear regression analysis (19).

The histogram distribution in Fig. 7*A* reports the relative frequencies of the $1/P_f$ increase, using a bin width of 0.2 units, in the three experimental conditions tested. Within this distribution, the C3 fusion toxin treatment indicated two peaks (R and N). *Peak R* (responding cells) is placed close to the peak resulting from forskolin treatment, and *peak N* is placed (nonresponding) below the data obtained from buffer-treated, i.e., resting, cells. The latter cells may represent a subpopulation of cells (N) that may be either nonresponding cells or cells not susceptible to the toxin. Figure 7*B* compares the absolute $1/P_f$ increase values in the three experimental conditions tested. Forskolin treatment resulted in an approximately twofold increase in P_f ($P < 0.05$, Fig. 7). In responding cells, the combination of C3 fusion toxin and C2II induces a significant increase in P_f comparable to that observed for forskolin stimulation (Fig. 7*B*; *peak R*).

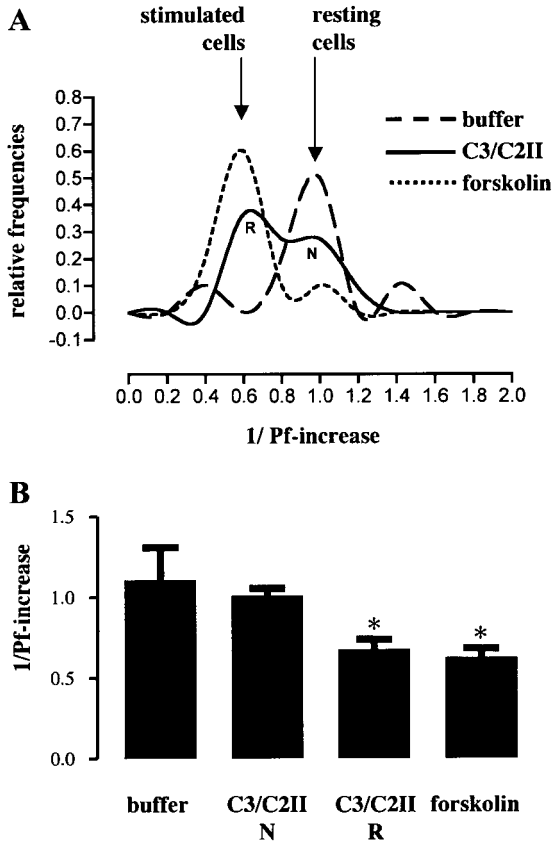

Fig. 7. Quantification of the increase in osmotic water permeability (P_f) of CD8 cells. Cells were left untreated (buffer), stimulated with forskolin (100 μM, 15 min), or with both C3 fusion toxin (100 ng/μl, 4 h) and the membrane-binding component C2II (200 ng/μl, 4 h). *A*: analysis depicting the relative frequency distribution of data obtained from single cells is shown. Binning was performed automatically using Graph Pad Prism. The majority of the CD8 cells analyzed respond to the fusion toxin (R), whereas a subpopulation did not respond to the toxin treatmemnt (N). *B*: the means ± SE of the inverse P_f increases ($6 < n < 10$) are shown. C3/C2II-treated responding cells (C3/C2II, R) displayed a P_f increase comparable to that observed after forskolin treatment ($P < 0.05$; unpaired Student's *t*-test).

Overall, these data suggest that the Rho family, and in particular Rho itself, regulates AQP2 insertion into the plasma membrane by altering F-actin-containing cytoskeletal structures.

DISCUSSION

The small GTP-binding proteins of the Rho family (Rho, Rac, and Cdc42) regulate F-actin-containing cytoskeletal structures. In this study, we demonstrate the involvement of small GTP-binding proteins of the Rho family in the translocation of AQP2 to the cell membrane in renal collecting duct CD8 cells.

Inactivation of all members of the Rho family by incubation with toxin B or selective inactivation of Rho by the combination of C3 fusion toxin and C2II induced the translocation of AQP2 to the apical membrane, in the absence of the cAMP-elevating stimulus forskolin. AQP2-bearing vesicles fused with the cell membrane, leading to a comparable increase in P_f values in response to either forskolin or C3 fusion toxin. The inhibition of the downstream effectors of Rho, the Rho kinases, induced a translocation of AQP2 to the cell membrane to a similar extent as the combination of C3 fusion toxin and C2II in the absence of forskolin. In agreement with those findings, expression of a constitutively active mutant of RhoA (RhoA-V14) abolished cAMP-mediated translocation of AQP2. These results indicate that the Rho family plays an inhibitory role in the AQP2 shuttle in renal collecting duct CD8 cells.

The inhibitory role of Rho in a cAMP-triggered exocytotic event (AQP2 translocation) has also been shown in primary cultured inner medullary collecting duct (IMCD) cells (13). These cells respond to vasopressin by a translocation of AQP2 predominantly to the lateral cell membrane (18). Treatment of IMCD cells with toxin B, C3 fusion toxin, or Y-27632 induced the translocation of AQP2 into the cell membranes in the absence of vasopressin. The effect of microinjection of IMCD cells with a plasmid encoding constitutively active RhoA-V14 prevented the cAMP-mediated translocation. Another study demonstrated that IMCD cells respond with a similar increase in P_f to toxin B treatment and to forskolin stimulation (19). These results are consistent with the data obtained for CD8 cells after the selective inactivation of Rho by C3 fusion toxin. The confimation of those findings in two cell culture models characterized by a different AQP2 sorting (apical vs. basolateral) is of particular value, as it indicates that the Rho-dependent signaling effect is independent from the specific sorting of the AQP2 to a defined membrane domain as well as from the origin of the cell line (either cortical or inner medullary collecting duct).

In CD8 cells, toxin B, the combination of C3 fusion toxin and C2II, and Y-26632 induced translocation of AQP2 to a similar extent (Fig. 3). These data suggest that within the family of Rho proteins, Rho appears to be fully responsible for the inhibitory effect in CD8 cells. None of the treatments led to translocation of AQP2 comparable to that obtained by forskolin stimulation, and forskolin further stimulated AQP2 translocation in toxin-pretreated cells (data not shown). The apparent submaximal translocation of AQP2 may be due to an incomplete inhibition of Rho. Alternatively, the presence of cells insensitive to C3 toxin treatment, as revealed by the biophysical responses in single CD8 cells, might mask a toxin effect on AQP2 translocation fully comparable to the forskolin effect.

In CD8 cells, we have previously shown that the serine/threonine phosphatase inhibitor okadaic acid increased the P_f independently of AQP2 phosphorylation in CD8 cells. Interestingly, CD8 cells treated with either forskolin or with okadaic acid showed actin depolymerizaton, indicating that reorganization of the F-actin cytoskeleton might be a prerequisite for promoting redistribution of AQP2-containing vesicles (30). In this respect, the findings reported in this work extend our knowledge on the involvement of the F-actin cytoskeleton in AQP2 translocation. Indeed, incubation of the cells with toxin B, C3 fusion toxin, and

Y-27632 resulted not only in AQP2 translocation but also in depolymerization of F-actin. Similarly, cytochalasin D caused both depolymerization of F-actin and translocation of AQP2 within 6–11 min of incubation. Thus F-actin depolymerization is sufficient to induce the translocation of AQP2. Conversely, induction of polymerization of F-actin by expression of constitutively active RhoA (RhoA-V14) abolished the translocation of AQP2 in response to forskolin in CD8 cells (Fig. 4). The increase in F-actin content may become a barrier, which apparently prevents translocation of AQP2-bearing vesicles to the cell membrane of resting cells. This hypothesis is supported by findings in other exocytotic processes. In chromaffin cells, pancreatic acinar cells, and mast cells, cortical F-actin disassembly before fusion of vesicles is considered a prerequisite for exocytosis (20, 21, 32, 33). Moreover, in alveolar epithelial type II cells, depolymerization of F-actin with C2 toxin increased basal surfactant secretion (23). The results presented here represent another example of how F-actin disassembly can trigger exocytosis and highlight the role of Rho in this context.

The emerging picture is that active Rho prevents AQP2 translocation from intracellular vesicles to the cell membrane, presumably by stimulating the formation of F-actin-containing cytoskeletal structures. As hormonal stimulation with vasopressin in collecting duct principal cells results in AQP2 translocation toward the apical membrane, we predict that under physiological conditions, Rho inhibition is one step of the signal transduction cascade triggered by vasopressin. Vasopressin-induced increases in intracellular cAMP cause PKA activation. Rho can be phosphorylated by PKA (16) at Ser^{188}, and this results in a decrease in the binding of RhoA to Rho kinase (6). The subsequent attenuation of Rho activity would favor depolymerization of F-actin, facilitating AQP2 insertion into the plasma membrane. As reported in this study, stimulation of CD8 cells with forskolin indeed induces a depolymerization of F-actin-containing cytoskeletal structures (Fig. 1). Further studies are in progress to elucidate intracellular pathways of Rho action in AQP2 targeting under physiological conditions.

In conclusion, the data presented here suggest that Rho activity is a key point of regulation of cAMP-triggered translocation to the apical membrane of AQP2, presumably through its role in actin cytoskeletal organization.

The authors thank Drs. G. Procino and M. Carmosino for valuable contributions to this work.

This work was supported by a grant from the EU-TMR network (proposal no. ERB 4061 PL 97–0406), by the Italian "Ministero della Ricerca Scientifica e Tecnologica", by the Vigoni program (1999–2001), and by the Deutsche Forschungsgemeinschaft (Ro 597/6).

REFERENCES

1. **Aspenstrom P.** The Rho GTPases have multiple effects on the actin cytoskeleton. *Exp Cell Res* 246: 20–25, 1999.
2. **Barth H, Hofmann F, Olenik C, Just I, and Aktories K.** The N-terminal part of the enzyme component (C2I) of the binary *Clostridium botulinum* C2 toxin interacts with the binding component C2II and functions as a carrier system for a Rho ADP-ribosylating C3-like fusion toxin. *Infect Immun* 66: 1364–1369, 1998.
3. **Brown D, Katsura T, and Gustafson CE.** Cellular mechanisms of aquaporin trafficking. *Am J Physiol Renal Physiol* 275: F328–F331, 1998.
4. **Brown D and Stow JL.** Protein trafficking and polarity in kidney epithelium: from cell biology to physiology. *Physiol Rev* 76: 245–297, 1996.
5. **Ding GH, Franki N, Condeelis J, and Hays RM.** Vasopressin depolymerizes F-actin in toad bladder epithelial cells. *Am J Physiol Cell Physiol* 260: C9–C16, 1991.
6. **Dong JM, Leung T, Manser E, and Lim L.** cAMP-induced morphological changes are counteracted by the activated RhoA small GTPase and the Rho kinase ROKalpha. *J Biol Chem* 273: 22554–22562, 1998.
7. **Hall A.** Rho GTPases and the actin cytoskeleton. *Science* 279: 509–514, 1998.
8. **Hays RM.** Cellular and molecular events in the action of antidiuretic hormone. *Kidney Int* 49: 1700–1705, 1996.
9. **Ishizaki T, Uehata M, Tamechika I, Keel J, Nonomura K, Maekawa M, and Narumiya S.** Pharmacological properties of Y-27632, a specific inhibitor of Rho-associated kinases. *Mol Pharmacol* 57: 976–983, 2000.
10. **Katsura T, Gustafson CE, Ausiello DA, and Brown D.** Protein kinase A phosphorylation is involved in regulated exocytosis of aquaporin-2 in transfected LLC-PK_1 cells. *Am J Physiol Renal Physiol* 272: F817–F822, 1997.
11. **Klussmann E, Maric K, and Rosenthal W.** The mechanisms of aquaporin control in the renal collecting duct. *Rev Physiol Biochem Pharmacol* 141: 33–95, 2000.
12. **Klussmann E, Maric K, Wiesner B, Beyermann M, and Rosenthal W.** Protein kinase A anchoring proteins are required for vasopressin-mediated translocation of aquaporin-2 into cell membranes of renal principal cells. *J Biol Chem* 274: 4934–4938, 1999.
13. **Klussmann E, Tamma G, Lorenz D, Weisner B, Maric K, Hofmann F, Aktories K, Valenti G, and Rosenthal W.** An inhibitory role of Rho in the vasopressin-mediated translocation of aquaporin-2 into cell membranes of renal pincipal cells. *J Biol Chem* 276(23): 20451–20457, 2001.
14. **Knepper MA and Inoue T.** Regulation of aquaporin-2 water channel trafficking by vasopressin. *Curr Opin Cell Biol* 9: 560–564, 1997.
15. **Kuwahara M, Fushimi K, Terada Y, Bai L, Marumo F, and Sasaki S.** cAMP-dependent phosphorylation stimulates water permeability of aquaporin-collecting duct water channel protein expressed in *Xenopus* oocytes. *J Biol Chem* 270: 10384–10387, 1995.
16. **Lang P, Gesbert F, Delespine-Carmagnat M, Stancou R, Pouchelet M, and Bertoglio J.** Protein kinase A phosphorylation of RhoA mediates the morphological and functional effects of cyclic AMP in cytotoxic lymphocytes. *EMBO J* 15: 510–519, 1996.
17. **Lerm M, Schmidt G, and Aktories K.** Bacterial protein toxins targeting Rho GTPases. *FEMS Microbiol Lett* 188: 1–6, 2000.
18. **Maric K, Oksche A, and Rosenthal W.** Aquaporin-2 expression in primary cultured rat inner medullary collecting duct cells. *Am J Physiol Renal Physiol* 275: F796–F801, 1998.
19. **Maric K, Wiesner B, Lorenz D, Klussmann E, Betz T, and Rosenthal W.** Cell volume kinetics of adherent epithelial cells measured by laser scanning reflection microscopy determination of water permeability changes of renal principal cells. *Biophys J* 80: 1783–1790, 2001.
20. **Muallem S, Kwiatkowska K, Xu X, and Yin HL.** Actin filament disassembly is a sufficient final trigger for exocytosis in nonexcitable cells. *J Cell Biol* 128: 589–598, 1995.
21. **Norman JC, Price LS, Ridley AJ, Hall A, and Koffer A.** Actin filament organization in activated mast cells is regulated by heterotrimeric and small GTP-binding proteins. *J Cell Biol* 126: 1005–1015, 1994.

22. **Price LS, Norman JC, Ridley AJ, and Koffer A.** The small GTPases Rac and Rho as regulators of secretion in mast cells. *Curr Biol* 5: 68–73, 1995.
23. **Rose F, Kurth-Landwehr C, Sibelius U, Reuner KH, Aktories K, Seeger W, and Grimminger F.** Role of actin depolymerization in the surfactant secretory response of alveolar epithelial type II cells. *Am J Respir Crit Care Med* 159: 206–212, 1999.
24. **Simon H, Gao Y, Franki N, and Hays RM.** Vasopressin depolymerizes apical F-actin in rat inner medullary collecting duct. *Am J Physiol Cell Physiol* 265: C757–C762, 1993.
25. **Sullivan R, Price LS, and Koffer A.** Rho controls cortical F-actin disassembly in addition to, but independently of, secretion in mast cells. *J Biol Chem* 274: 38140–38146, 1999.
26. **Uehata M, Ishizaki T, Satoh H, Ono T, Kawahara T, Morishita T, Tamakawa H, Yamagami K, Inui J, Maekawa M, and Narumiya S.** Calcium sensitization of smooth muscle mediated by a Rho-associated protein kinase in hypertension. *Nature* 389: 990–994, 1997.
27. **Valenti G, Frigeri A, Ronco PM, D'Ettorre C, and Svelto M.** Expression and functional analysis of water channels in a stably AQP2-transfected human collecting duct cell line. *J Biol Chem* 271: 24365–24370, 1996.
28. **Valenti G, Hugon JS, and Bourguet J.** To what extent is microtubular network involved in antidiuretic response? *Am J Physiol Renal Fluid Electrolyte Physiol* 255: F1098–F1106, 1988.
29. **Valenti G, Procino G, Carmosino M, Frigeri A, Mannucci R, Nicoletti I, and Svelto M.** The phosphatase inhibitor okadaic acid induces AQP2 translocation independently from AQP2 phosphorylation in renal collecting duct cells. *J Cell Sci* 113: 1985–1992, 2000.
30. **Valenti G, Procino G, Liebenhoff U, Frigeri A, Benedetti PA, Ahnert-Hilger G, Nurnberg B, Svelto M, and Rosenthal W.** A heterotrimeric G protein of the Gi family is required for cAMP-triggered trafficking of aquaporin 2 in kidney epithelial cells. *J Biol Chem* 273: 22627–22634, 1998.
31. **Van Aelst L and D'Souza-Schorey C.** Rho GTPases and signaling networks. *Genes Dev* 11: 2295–2322, 1997.
32. **Vitale ML, Seward EP, and Trifaro JM.** Chromaffin cell cortical actin network dynamics control the size of the release-ready vesicle pool and the initial rate of exocytosis. *Neuron* 14: 353–363, 1995.
33. **Vitale N, Gasman S, Caumont AS, Gensse M, Galas MC, Chasserot-Golaz S, and Bader MF.** Insight in the exocytotic process in chromaffin cells: regulation by trimeric and monomeric G proteins. *Biochimie* 82: 365–373, 2000.
34. **Wade JB, Stetson DL, and Lewis SA.** ADH action: evidence for a membrane shuttle mechanism. *Ann NY Acad Sci* 372: 106–117, 1981.